Molecular coatings improve the selectivity and durability of CO_2 reduction chalcogenide photocathodes

Yungchieh Lai[1], Nicholas B. Watkins[2], Christopher Muzzillo[3], Matthias Richter[1], Kevin Kan[1], Lan Zhou[1], Joel A. Haber[1], Andriy Zakutayev[3], Jonas C. Peters[2,*], Theodor Agapie[2,*], John M. Gregoire[1,*]

[1] Division of Engineering and Applied Science, California Institute of Technology, Pasadena, CA, USA

[2] Division of Chemistry and Chemical Engineering, California Institute of Technology, Pasadena, CA, USA

[3] Materials Science Center, National Renewable Energy Laboratory, Golden, CO, USA

[*]E-mail: gregoire@caltech.edu (J.M.G.), agapie@caltech.edu (T.A.), jpeters@caltech.edu (J.C.P.)

Supporting Information

Experimental Methods

Photocathode synthesis

$CuGa_3Se_5$ absorbers were deposited on soda-lime glass substrates with Mo back contact deposited by sputtering. The deposition was performed at 600 °C using a three-stage co-evaporation process, with Ga-Se sourced in the 1st stage, Cu-Se sourced in the 2nd stage, and Ga-Se sourced in the 3rd stage. The solution for CdS deposition contained 1.2 mM of cadmium sulfate ($CdSO_4$) and 59 mM of thiourea (CH_4N_2S) in NH_4OH and DI water, and was heated to 65°C during the coating process. More details about these experiments can be found in prior publications.[24,25]

Additive synthesis and characterization

Additives were synthesized according to previously published procedures using chemicals as received from commercial suppliers without further purification.[32,33]

High throughput electrochemical testing

Prior to the electrolysis, the electrolyte (0.1 M $KHCO_3$, ≥99.95% trace metals basis, Sigma Aldrich) with or without additives (**Add. 1** or **Add. 2**) was purged with CO_2 (99.999%, Airgas) for at least 30 min. A bipolar membrane (BPM, Fumasep® FBM single film, Fumatech) was used to separate the working and counter electrodes. Platinum wire (99.9%, Sigma Aldrich) was used as the counter electrode. Electrolysis was carried out with a Gamry Reference 600TM potentiostat. All electrochemical data were collected using a Ag/AgCl reference electrode (LF2, Innovative Instruments) and converted to a reversible hydrogen electrode (RHE) scale using the measured solution pH of 6.8. All cells and all solution handling lines were purged with fresh electrolyte and CO_2 between electrolysis to avoid cross-contamination. These systems were coupled with front-side electrode illumination using fiber-coupled LEDs. The surface area of the counter electrodes were about 0.25 cm^2, while the working electrode surface areas were 0.32 cm^2. The flow rate of electrolyte was 160 µL/s throughout the tests.

Two cell designs were used for the bulk testing of photocathodes.

(1) An electrochemical mass spectrometry (ECMS) system was previously published for rapid CO2R electrocatalyst screening.[43] Mass spectra were acquired on a Hiden HPR20 mass spectrometer connected to the outlet of the desiccant chamber. An electron energy of 70 eV was used for ionization of all species,

with an emission current of 500 μA to maximize detection sensitivity. Hydrogen (m/z = 2), methane (m/z = 15), and ethylene (m/z = 26) ions were accelerated with a voltage of 3 V. All mass-selected product cations were detected by a secondary electron multiplier with a detector voltage of 1050 V.

(2) Analytical and Electro-chemistry (HT-ANEC) is an analytical electrochemistry system previously published by our group to efficiently detect a wide range of CO_2R products.[37] At the end of each (photo)electrolysis, gaseous and liquid products were sampled by the robotic sample handling system (RSHS) and analyzed by GC (Thermo Scientific™ TRACE™ 1300) and HPLC (Thermo Scientific UltiMate 3000). Detailed product detection (method) can be found at the previous publication.[37]

H-cell electrochemical testing

For photoelectrochemical CO_2 reduction durability experiments in an H-Cell a custom peek cell was utilized.[44] The anode and membrane had an area of 1 cm^2 whereas the area of the cathode was further reduced by a Viton mask to 0.5 cm^2. CO_2 saturated 0.10 M potassium bicarbonate with and without additive was used as the electrolyte. A Pt foil anode was used behind a bipolar membrane (Fumasep® FBM single film, Fumatech) membrane. A leakless Ag/AgCl electrode was used as a reference electrode. A monochromatic LED illumination with a wavelength of 450 nm and an intensity of 65 mW/cm^2 was used.

Carbon dioxide was provided to the electrochemical cell at a flow rate of 5 sccm as controlled by an Alicat flow controller. The gas stream was humidified by a gas bubbler connected in series between the electrochemical cell and flow controller. The gas exhaust stream of the electrochemical cell was passed through a liquid trap before flowing through the gas sampling loop of an Agilent 7820a GCMS/TCD with an Alicat flow meter connected to its exhaust. Quantitative analysis of gaseous products was based on calibrations with several gas standards over many orders of magnitude in concentration. With the help of the calibration, the Faradaic efficiency towards CO2R and hydrogen evolution products could be calculated from the measured current density. For isotope labeling experiments the same experimental configurations as described above were employed except $^{13}CO_2$ was used as the CO_2 source.

Pre- and post- (photo)electrochemistry sample characterization

TEM/EDS

Cd(S) layer in $CdS/CuGa_3Se_5$ at different conditions was characterized by cross-sectional Transmission electron microscopy (TEM) and energy-dispersive X-ray spectroscopy (EDS). To prepare a cross-sectional TEM specimen, a FEI DualBeam Focused Ion Beam/scanning electron microscope (FIB/SEM) was used and the sample was capped carbon/I-C prior to milling. TEM experiments were carried out in a FEI Tecnai Osiris FEG/TEM operated at 200 kV in bright-field (BF) and high-resolution (HR) TEM mode. The EDX elemental mapping was acquired using Bruker Quantax. This characterization was performed by Eurofins EAG Precision TEM in Santa Clara, California.

XRF and ICP-MS

The Cd in $CdS/CuGa_3Se_5$ sample was characterized by X-ray fluorescence (XRF) using an EDAX Orbis Micro-XRF system to identify if any was leached out during the photo(electrochemistry) measurements. Inductively coupled plasma mass spectrometry (ICP-MS) by Thermo Fisher Scientific iCAP™ RQ instrument was used to determine the concentration of dissolved metals in electrolytes used for electrochemistry.

SEM

Morphology of the Cd(S) layer and additives were characterized by Cross-sectional and top-down view Scanning-electron microscopy images and were obtained with a FEI Nova NanoSEM 450 microscope.

XPS

X-ray photoelectron spectroscopic (XPS) data were collected using a Kratos Axis Nova system with a base pressure of 1×10^{-9} Torr. The X-ray source was a monochromatic Al Kα line at 1486.6 eV. Photoelectrons were collected at 0° from the surface normal with a retarding pass energy of 160 eV for survey XPS scans with a step size of 0.5 eV, and a pass energy of 20 eV for high-resolution core level scans with a step size of 0.05 eV. No charge neutralization was used. The XPS was calibrated using the Au $4f_{7/2}$ line (84 eV) of a sputtered gold foil. Data was analyzed using CasaXPS. To calculate the composition (atomic ratio) a Shirley background was subtracted. The core level intensities were corrected by the analyzer transmission function and relative sensitivity factors to obtain corrected peak intensities which were used to calculate the atomic ratios.

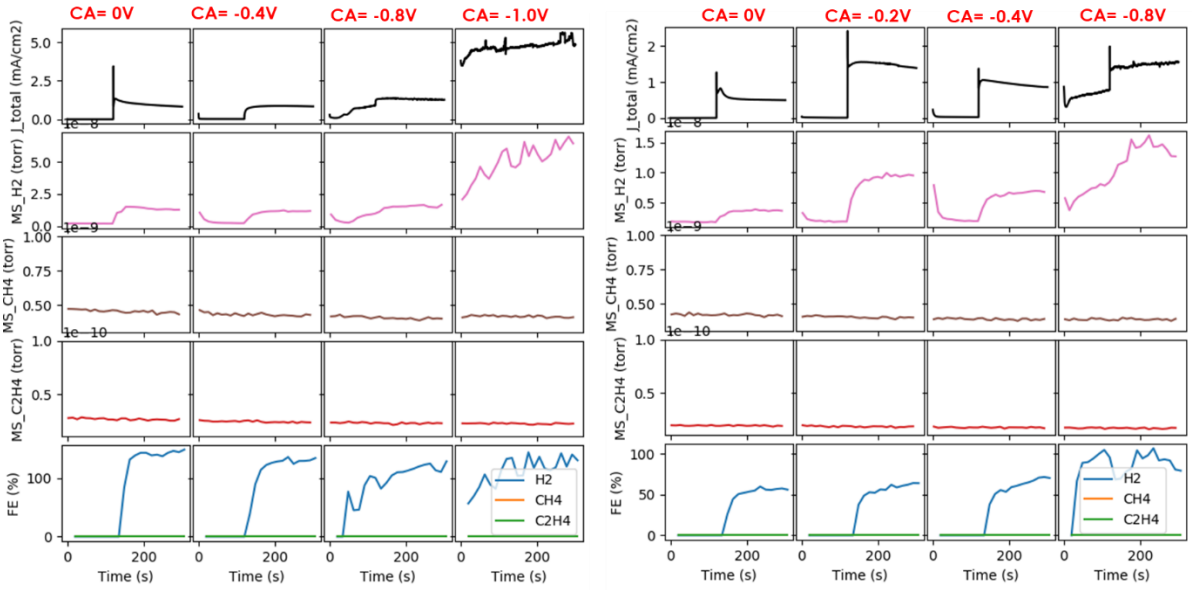

Figure S1: Initial experiments in an electrochemical flow cell where for each of 2 electrodes without (left) and with (right) CdS coating were operated as a sequence of applied bias, chronologically from left to right. At each potential, after 120 s operation in the dark illumination from a 455 nm LED was used to observe any photocurrent and change in H_2, CH_4, and C_2H_4 production rate, which were quantified using mass spectrometry via a pervaporation cell in the effluent of the electrolyte from the electrochemical reactor. Both samples show negligible dark current and appreciable photocurrent from 0 to -0.4 V vs RHE with undesirably large dark current at more negative bias. While no hydrocarbons are observed, the observed H_2 signal is used to estimate the Faradaic efficiency, which is near 100% without the CdS coating and is lower with CdS, indicating formation of a non-detected product such as CO or another electrochemical reaction occurring.

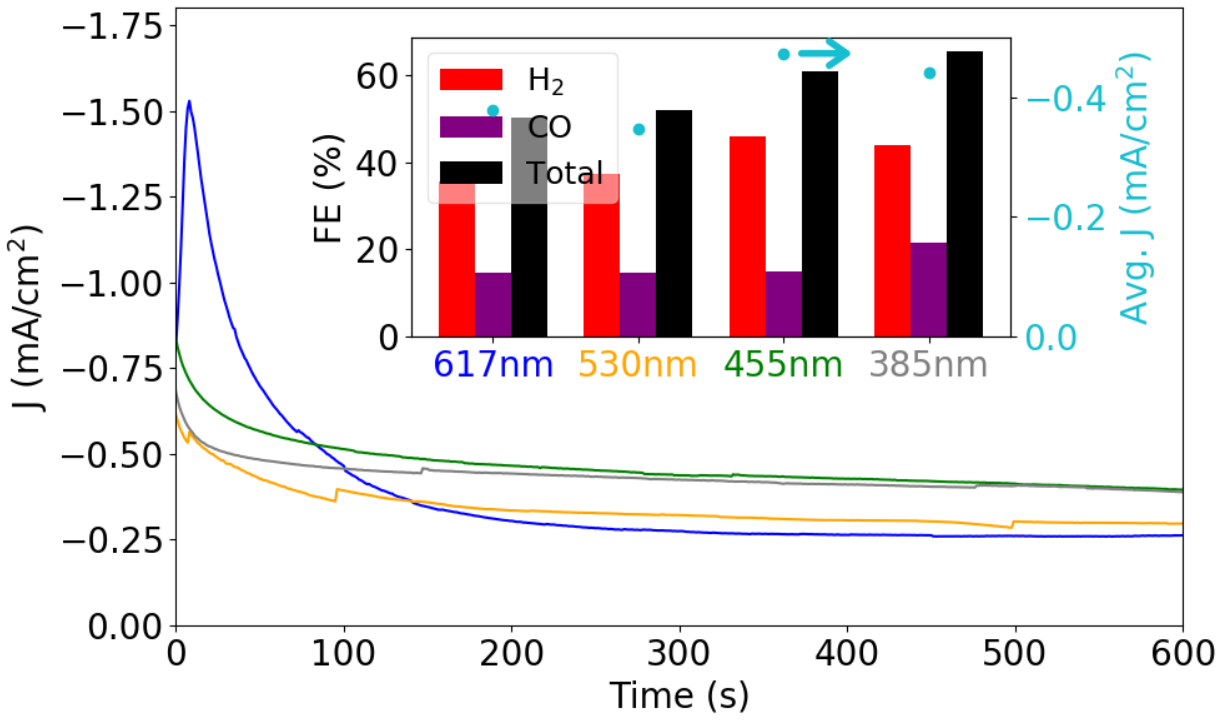

Figure S2: Evaluation of the product distribution with illumination ranging from 617 nm to 385 nm at 0V vs RHE. The testing sequence is 617, 530, 455, and then 385nm. The FE, especially for CO, is similar for the first 3 illumination sources and increases at 385 nm illumination. The 455 nm illumination was chosen for further experimentation to represent visible illumination. Note that xrf was used to monitor the Cd corrosion with 81 (counts) prior to test and 14.5 (counts) after photoelectrolysis with the four wavelengths.

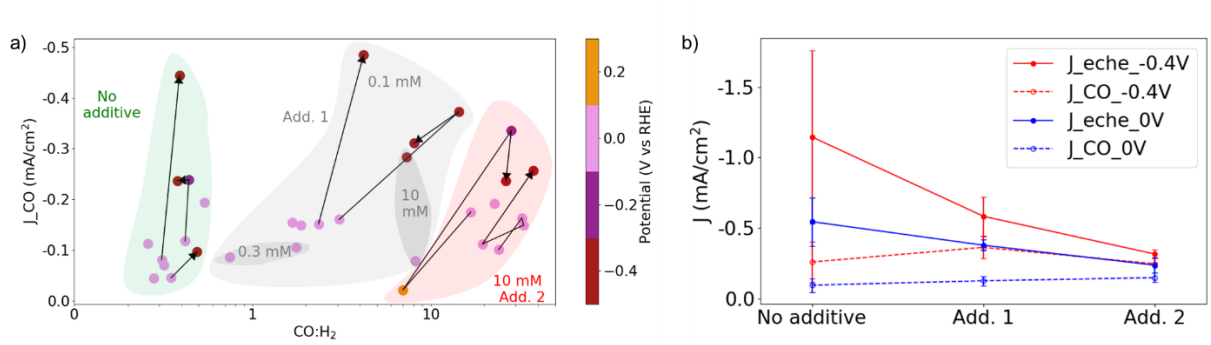

Figure S3: a) The data from Figure 2 is shown using the partial current density for CO as opposed to the total current density, and multiple experiments on a given electrode are shown with arrows indicating the sequence of measurements. b) Aggregation of the experiments in a) for the -0.4 and 0V, indicating that the primary mechanism of selectivity enhancement with the additives is suppression of HER. The error bars for both J_eche and J_CO at -0.4 V and 0 V vs RHE represent the standard deviation of the respective measurements over the several photoelectrocatalysis experiments shown in a).

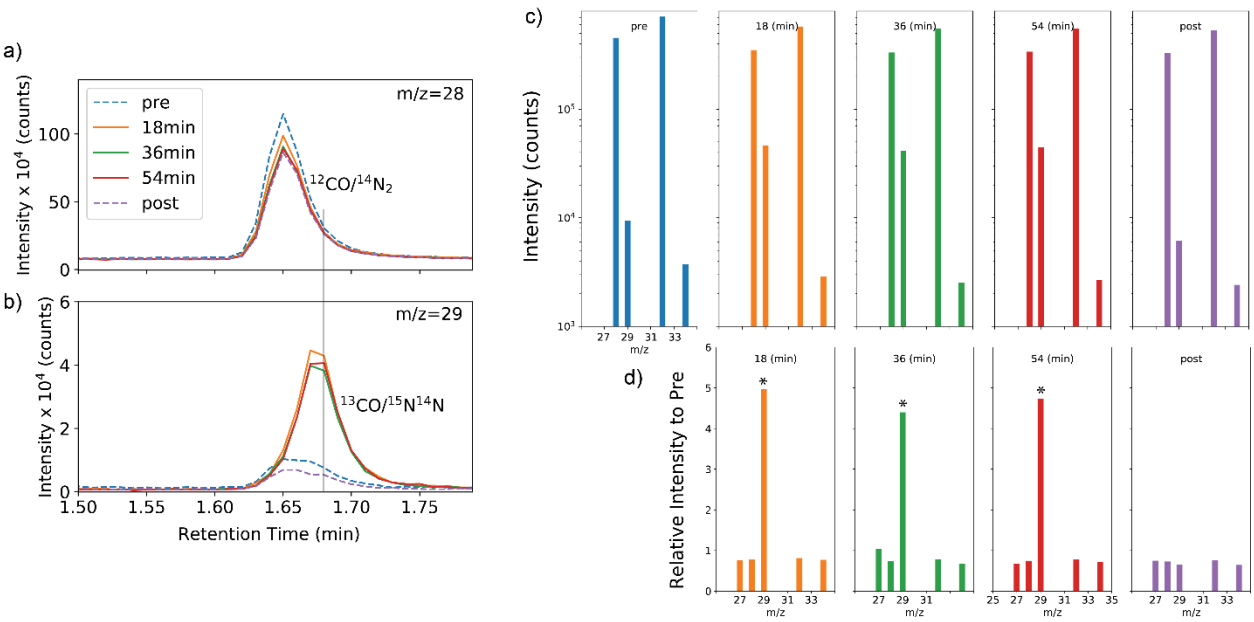

Figure S4: GC-MS analyses with isotopically-labelled $^{13}CO_2$ with aliquots acquired before ("pre"), at 3 time intervals during photoelectrolysis at 0 V vs RHE with 10 mM **Add. 2**, and after photoelectrolysis ("post"). For each of these 5 headspace samples, mass spectra were acquired at a series of GC retention times. The 2 m/z values of interest are 28 and 29, which correspond to ^{12}CO and ^{13}CO, respectively, the latter being the target product of photoelectrochemical reduction of $^{13}CO_2$. The N_2 from air contamination has similar retention time as that of CO and contributes to both a) m/z= 28 and b) m/z=29 signals as shown in the "pre" and "post" measurements. The mass spectrum acquired at 1.68 min retention time, marked with a vertical gray line in a) and b), best characterizes CO with some contribution from N_2. For each of the 5 conditions, the relevant portion of the mass spectrum is shown in c) where the colors match the legend in a). To compare the signals during photoelectrolysis to those of the "pre" baseline, d) contains the relative intensity for each m/z value with detected intensity. The approximately 5-fold enhancement in m/z=29 signal in each of the measurements during photoelectrolysis is marked with an asterisk. As shown in a), the m/z=28 "pre" signal, which is from $^{14}N_2$, is similar to the m/z=28 signals in subsequent measurements. The concomitant m/z=29 signal from $^{15}N^{14}N$ is thus also similar in each measurement, demonstrating that the ~5-fold increase in m/z=29 signal for the measurements during photoelectrolysis arises from photoelectrochemical generation of ^{13}CO from $^{13}CO_2$.

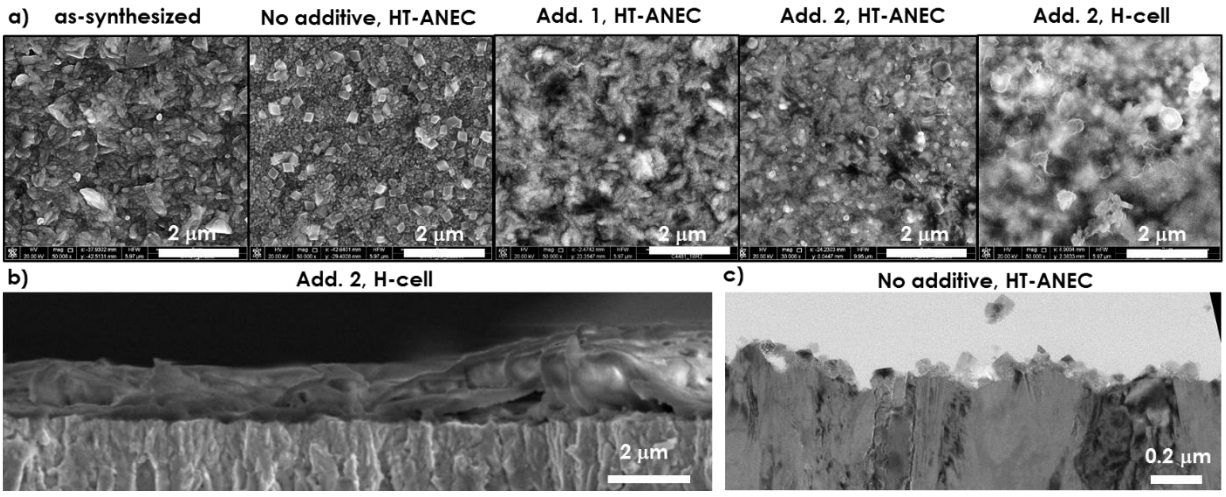

Figure S5: a) Plan-view SEM images of electrodes including as-synthesized, each condition from the HT-ANEC measurements of Figure 2, and the H-cell measurement of Figures 3b-3c. b) Cross-sectional SEM for H-cell with **Add. 2**, which shows variations in the film thickness. c) Cross-section TEM image of an electrode from HT-ANEC without additive. With no additive, the surface restructures into nanocubes. The images from experiments with a molecular additive exhibit a morphology that is more similar to the as-synthesized electrode with some apparent restructuring and/or changes in morphology due to heterogeneities in organic coating.

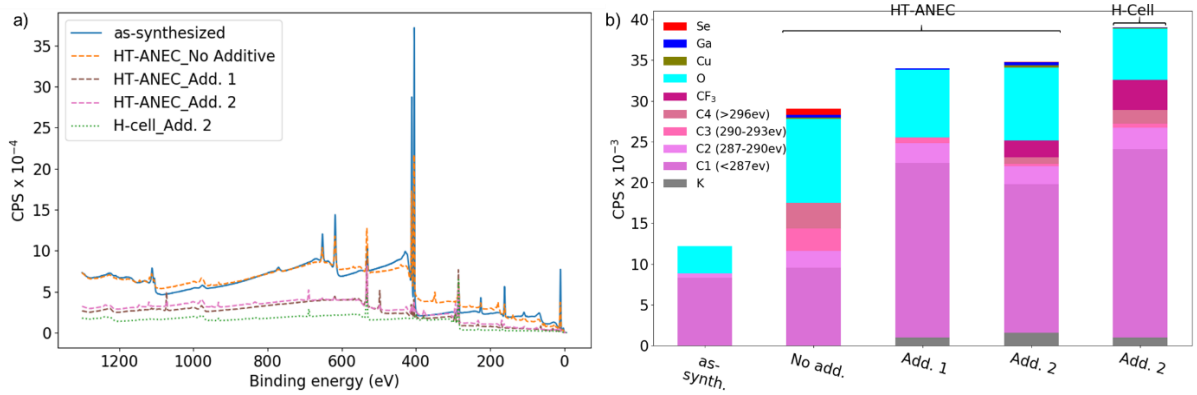

c)

Sample	C 1s1	C 1s2	C 1s3	C 1s4	C 1s CF3	Cd 3d	Cu 2p	Ga 2p	K 2p 1	N 1s	O 1s	S2p 1	S2p 2	Se3d	Se3p
as-synthesized	8310	557	0	0	0	6520	0	0	0	187	3340	5570	278	0	0
No additive	9560	2030	2760	3180	0	4750	153	300	0	353	10300	2100	0	783	719
Add. 1, HT-ANEC	21400	2440	691	0	0	593	6.43	131	987	1340	8320	292	848	23.7	24
Add. 2, HT-ANEC	18200	2190	278	838	2070	345	280	374	1600	2520	8900	595	1230	64.5	62.8
Add. 2, H-cell	23100	2640	473	1700	3640	0	129	44.7	1000	2740	6310	130	263	16.1	0

Figure S6: a) XPS survey scans for the 5 electrode conditions of Figures 4a-4b. The analysis of the detected species from each electrode are shown in b) and Figure 4c. All samples that underwent electrochemistry have a signal near a binding energy of 293 eV that is likely from precipitates of KCO_3 from the electrolyte. The samples with **Add. 2** also show F and C signals corresponding to CF_3, which is the counterion in the molecular additive (the CPS of the corresponding C 1s peak is shown in b), which may also result from precipitates of the electrolyte. Adventitious carbon and the molecular additive

both contribute to C1, C2 can be assigned to carbonate species (CO_3), C3 and C4 are satellite and shake-up peaks. c) The summary of all quantified XPS peaks that provide the basis for Figure 4c and b). The N:Cd is 7.3 after the 10 min HT-ANEC operation with Add. 2. After the H-cell measurement included 3.3 h without additive, the N signal is slightly higher and the Cd signal is below the detectability limit, indicating that the N:Cd ratio is above 100. These results are commensurate with the microscopy images of Figure 4 that show a conformal and thick additive coating after the H-cell measurements.

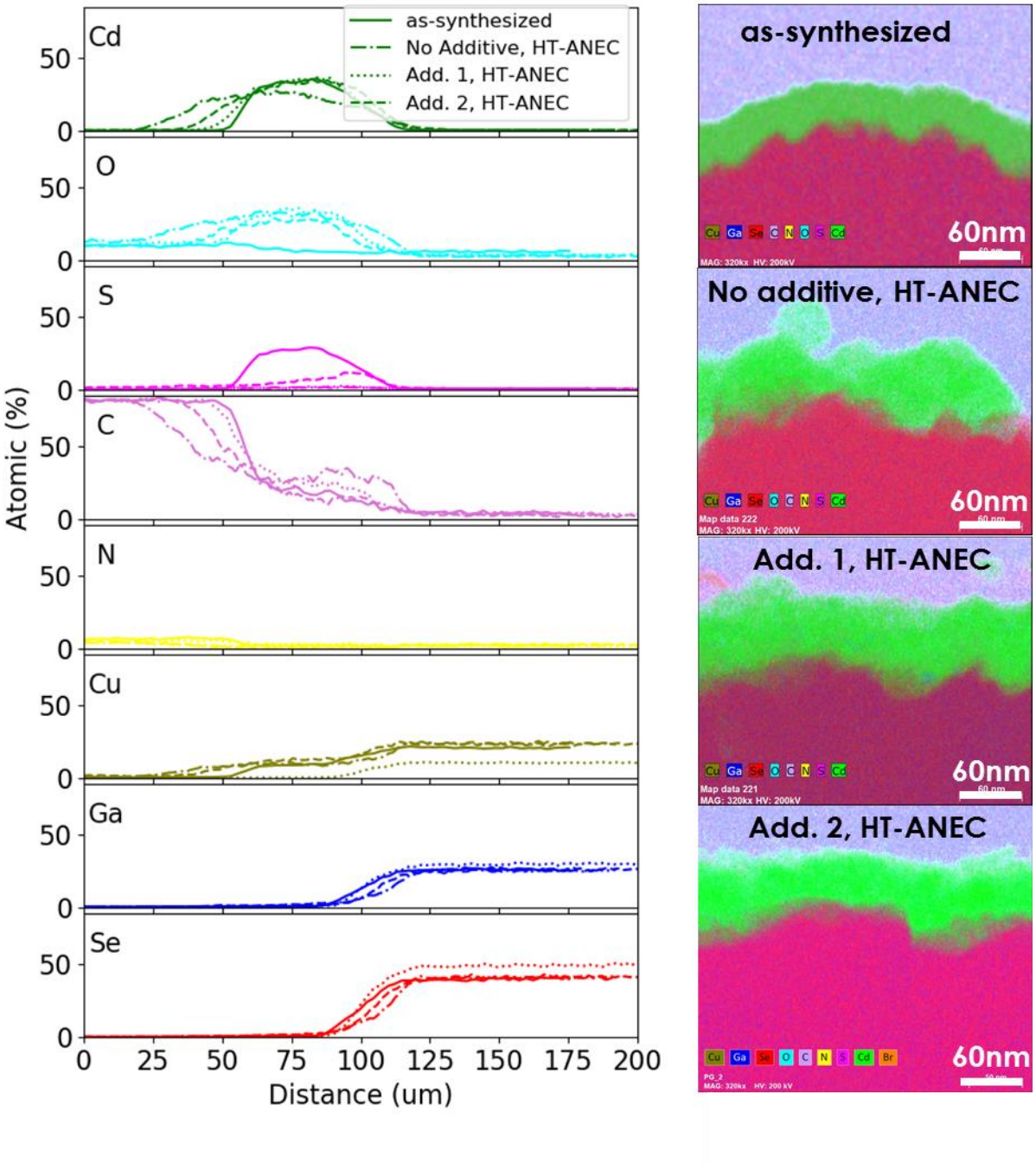

Figure S7: Additional TEM data supporting Figure 4b. The depth profile of elemental composition is obtained by horizontal averaging of the EDS mapping images for each sample.

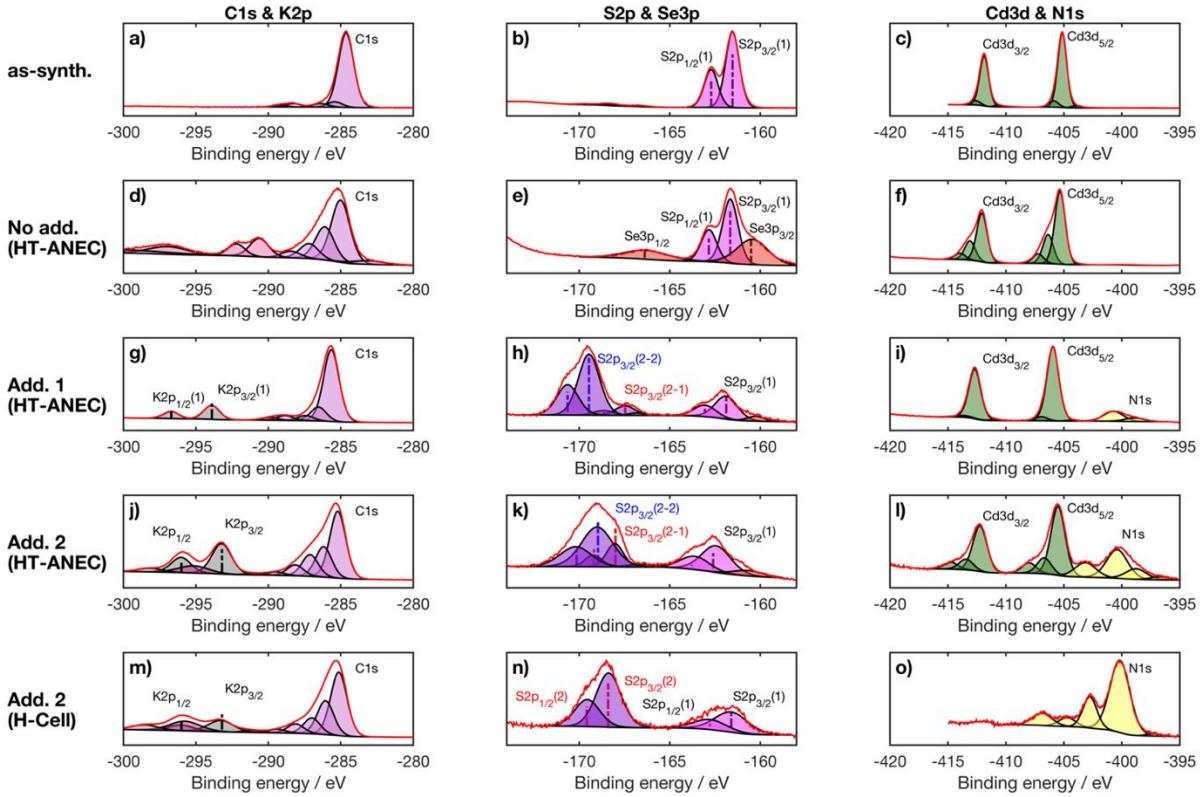

Figure S8: High resolution core level spectra for the energy regions containing C 1s and K 2p (a, d, g, j, m), S 2p and Se 3p (b,e, h, k, n) and Cd 3d and N 1s (c, f,i,l,o) core levels. The N originating from the additive molecules is also apparent in the respective samples. XPS signals from the as-synthesized and no-additive samples include an S $2p_{3/2}$ binding energy near 161.5 eV ($S_{sulfide}$ in Figure 4c), as expected for a CdS.[45] The electrodes with additive show an additional S signal with $2p_{3/2}$ binding energy of 168-169 eV ($S_{sulfate}$ in Figure 4c), which is more characteristic of sulfate species.[46–48] In the **Add. 1** sample, this signal may arise from $CdSO_4$ from oxidation of the CdS layer, although the low Cd signal may suggest some sulfate complexation in the molecular coating, which initially contains no sulfur. In the **Add. 2** samples, this signal may arise from the triflate counterion to the molecular additive. The C 1s signal involves multiple components whose intensities vary with condition (Figure S5), although the multiple sources of carbon from the electrolyte, additive, and adventitious sources preclude detailed interpretation at this time. The XPS signals collectively corroborate the findings from electron microscopy and provide guidance for future detailed exploration of the chemistry.

Table S1: The photocurrent and product distribution, as well as XRF and ICP-MS characterization of Cd corrosion, from each electrolysis experiment tested with 455 nm LED (450nm LED for H-cell tests). The measured Cd concentration prior to (photo)electrolysis by ICP-MS ranges between 0-4 ppb, which is within the detectability limit. The Cd characterized by XRF prior to photoelectrolysis is 80 ± 6 (counts) and for post-run characterization it is only conducted after all photo-electrolysis on a sample are completed.

Sample spot	Add. type	Add. conc. (mM)	Poten. (V vs RHE)	J_eche (mA/cm^2)[d]	FE_H_2 (%)	FE_CO (%)	Cd, pre (ppb)[a]	Cd, post (ppb)[b]	Cd, XRF (counts)[c]
1	N/A	N/A	0	-0.32	41.1	14.3	N/M	N/M	N/M
1	N/A	N/A	-0.4	-0.47	41.7	20.4	N/M	N/M	31
2	N/A	N/A	0	-0.82	43.8	23.6	N/M	N/M	9.2
3	N/A	N/A	0	-0.47	45.9	14.9	N/M	N/M	15
4	N/A	N/A	0	-0.5	51.3	16.0	N/M	N/M	N/M
4	N/A	N/A	-0.4	-1.96	58.5	22.7	N/M	N/M	5
5	N/A	N/A	0	-0.57	49.2	20.7	4.2	45.53	N/M
5	N/A	N/A	-0.2	-0.98	55.4	24.4	4.2	38.06	N/M
5	N/A	N/A	-0.4	-1.01	60.9	23.5	4.2	40.94	19
6	N/A	N/A	0	-0.38	42.0	11.9	2.9	39.05	68
7	N/A	N/A	0	-0.76	56.7	14.9	0	30.59	69
8	**Add. 1**	0.1	0	-0.38	13.8	42.4	N/M	N/M	N/M
8	**Add. 1**	0.1	-0.4	-0.54	4.8	69.5	N/M	N/M	N/M
8	**Add. 1**	0.1	-0.4	-0.5	7.6	61.7	N/M	N/M	22
9	**Add. 1**	0.1	0	-0.38	17.0	39.8	5.3	3.88	N/M
9	**Add. 1**	0.1	-0.4	-0.82	14.1	59.2	5.3	23.13	N/M
10	**Add. 1**	0.1	0	-0.44	20.8	34.9	6.8	28.20	67
11	**Add. 1**	0.1	0	-0.41	19.3	36.2	2.9	4.27	74
12	**Add. 1**	0.3	0	-0.35	17.3	30.4	4.4	32.50	60
13	**Add. 1**	0.3	0	-0.38	30.4	22.7	1.5	48.70	52
14	**Add. 1**	10	0	-0.32	3.0	24.8	3.6	37.13	64
15	**Add. 1**	10	-0.4	-0.47	8.2	59.9	3.6	0.58	54
16	**Add. 2**	10	0	-0.28	3.0	67.4	6.59	4.08	82
17	**Add. 2**	10	0	-0.19	2.2	53.2	1.32	0.76	N/M
17	**Add. 2**	10	0	-0.25	2.0	64.6	1.32	0.57	N/M
17	**Add. 2**	10	0	-0.22	2.0	67.5	1.32	0.46	N/M
17	**Add. 2**	10	0	-0.16	3.6	70.9	1.32	0.36	N/M
17	**Add. 2**	10	-0.4	-0.35	2.0	74.0	1.32	0.31	83
18	**Add. 2**	10	0	-0.32	3.3	55.4	0.73	0.46	N/M
18	**Add. 2**	10	0.2	-0.06	4.9	34.0	0.73	0.59	N/M
18	**Add. 2**	10	-0.2	-0.44	2.7	75.9	0.73	0.17	N/M
18	**Add. 2**	10	-0.4	-0.28	3.2	83.3	0.73	0.32	82
19[e]	**Add. 2**	10	0	-0.13	8.7	53.9	N/M	N/M	N/M
19[f]	N/A	N/A	0	-0.13	14.0	51.0	N/M	0.23	79

N/A: not applicable; N/M: not measured; a) Pre-PEC electrolyte measured for Cd by ICP-MS and it is only measured once prior to 1st PEC of each sample spot; b) Post-PEC electrolyte measured for Cd by ICP-MS; c) Post-PEC sample measured for Cd by XRF; d) Averaged J_eche current during the CA period; e) First 1.2 hour of stability test by H-cell from figure 3b; f) Continued 3.3 hour of stability test by H-cell from Figure 3c